Chemical Engineering Journal 162 (2010) 158–163

Contents lists available at ScienceDirect

Chemical Engineering Journal

journal homepage: www.elsevier.com/locate/cej

Surface chemical modification on hyper-cross-linked resin by hydrophilic carbonyl and hydroxyl groups to be employed as a polymeric adsorbent for adsorption of *p*-aminobenzoic acid from aqueous solution

Xiaomei Wang [a], Jianhan Huang [b,*], Kelong Huang [b]

[a] *Department of Bioengineering and Environmental Science, Changsha University, Changsha 410003, China*
[b] *School of Chemistry and Chemical Engineering, Central South University, Changsha 410083, China*

ARTICLE INFO

Article history:
Received 2 April 2010
Received in revised form 9 May 2010
Accepted 10 May 2010

Keywords:
Surface chemical modification
Hyper-cross-linked resin
Adsorption
Hydrogen bonding

ABSTRACT

In this study, a novel hyper-cross-linked HJ-Y10 resin was synthesized and its adsorption behaviors for *p*-aminobenzoic acid were investigated from aqueous solution. The results indicated that the skeleton surface of HJ-Y10 resin was modified by formaldehyde carbonyl, quinone carbonyl and phenolic hydroxyl groups, the unadjusted *p*-aminobenzoic acid solution was favorable for the adsorption, the isotherms could be fitted by Langmuir model and the adsorption was an exothermic process, the adsorption kinetics could be characterized by pseudo-second-order rate equation and the initial stage was controlled by the intra-particle diffusion model. Hydrogen bonding between formaldehyde carbonyl, quinone carbonyl groups on HJ-Y10 resin and carboxyl groups of *p*-aminobenzoic acid was one of the primary driving forces for the adsorption.

1. Introduction

p-Aminobenzoic acid is a new vitamin in family of vitamin B, it can keep the skin lubricative, retard appearance of wrinkle and obstruct sun's rays [1,2]. Also, *p*-aminobenzoic acid is often used in industry as an organic intermediate to produce dyes like active read M-80, M-10B and medicines like *p*-carboxylbenzyl amine, *p*-cyanobenzoic acid. Therefore, developing efficient methods to separate and purify *p*-aminobenzoic acid is very important.

Adsorption is an effective method for purification of aromatic compounds [3,4] and the well-known adsorbent applied in adsorption is activated carbon, which has high specific surface area and predominant micropores to endow them with large adsorption capacity for aromatic compounds [5]. Nevertheless, how to regenerate the spent activated carbon effectively for repeated use is a serious problem. Correspondingly, synthetic polymeric adsorbents are gradually attractive due to their diverse surface chemical structure and feasible regeneration for repeated use [6–9].

In the 1970s, Davankov synthesized a kind of hyper-cross-linked polystyrene resin using bi-functional cross-linking agents and Friedel-Crafts catalysts from linear polystyrene or low cross-linked poly(styrene-co-divinylbenzene) (PS) [10,11]. Then a large number of rigid methylene bridges are formed between the polymeric chains according to this method and hence the polymeric skeleton is reinforced. Moreover, the specific surface area of the obtained resins increases greatly, and mesopores in the range of 2–10 nm predominate their pore structure, resulting in their excellent adsorption behaviors for non-polar or weak polar aromatic compounds [12,13]. To improve their adsorption properties for polar aromatic compounds, three techniques are frequently employed, the introduction of polar unit in copolymers [14], the employment of polar compound as the cross-linking reagent [15] and the addition of polar aromatic compound in Friedel-Crafts reaction [16,17]. As the prepared resins are tested for solid-extraction of polar aromatic compound, it is found that their retention is improved [18,19]. If macroporous low cross-linked chloromethylated PS is applied as the reactant, anhydrous zinc chloride is used as the Friedel-Crafts catalyst, and hydroquinone is added into the reaction simultaneously, two possible reactions will arise, one is the Friedel-Crafts reaction of chloromethylated PS itself and the other is that of chloromethylated PS with hydroquinone. The respective extent of the two reactions will determine the structure and adsorption behaviors of the gained resin. However, no report focuses on the synthesis of hydroquinone modified hyper-cross-linked resin and the study of their adsorption properties.

Hydrogen bonding, as a specifically intramolecular or intermolecular interaction [20], is proven to be one of the most important adsorption mechanisms for adsorption of aromatic compounds onto resins from aqueous or non-aqueous solution [21,22]. Many literatures reported the synthesis of resins based on hydrogen bonding [23–25], and adsorption mechanism on basis of

* Corresponding author at: School of Chemistry and Chemical Engineering, Central South University,Changsha 410083, China. Fax: +86 731 88879616.
E-mail address: xiaomeijiangou@yahoo.com.cn (J. Huang).

1385-8947/$ – see front matter © 2010 Elsevier B.V. All rights reserved.
doi:10.1016/j.cej.2010.05.017

hydrogen bonding is usually clarified by thermodynamic or theoretical calculation [26–28]. To the best of our knowledge, direct evidence to testify hydrogen bonding between the resin and the adsorbate is little discussed [29].

This work aimed at surface chemical modification of macroporous cross-linked chloromethylated PS by adding hydroquinone in Friedel-Crafts reaction. The pore structure, surface chemical structure and adsorption behaviors of the synthesized resin were thereafter studied. HJ-Y10 resin was selected as the resin, *p*-aminobenzoic acid was chosen as the adsorbate, and the adsorption behaviors of HJ-Y10 were investigated to prospect its potential application in adsorption of *p*-aminobenzoic acid. Its adsorption thermodynamics and kinetics were analyzed and adsorption mechanism was directly expounded by Fourier-transform infrared ray (FT-IR) spectra.

2. Materials and methods

2.1. Materials

Macroporous cross-linked chloromethylated PS was purchased from Langfang Chemical Co. Ltd. (Hubei province, China), its cross-linking degree was 6%, chlorine content was 17.3%, specific surface area was 28 m^2/g, and average pore diameter was 25.2 nm. Hydroquinone, *p*-aminobenzoic acid, anhydrous zinc chloride, nitrobenzene and ethanol were also used in this study and they were analytical reagents.

2.2. Surface chemical modification of macroporous cross-linked chloromethylated PS

Surface chemical modification of macroporous cross-linked chloromethylated PS was performed according to the method in ref [17] and its synthetic process was shown in Scheme 1s. In a three-necked round-bottomed flask equipped with a mechanical stirrer, a thermometer and a water-cooled condenser, 40 g of chloromethylated PS was swollen by 120 mL of nitrobenzene, and 4 g of hydroquinone was also added into the reaction flask. At a moderate stirring speed, 4 g of anhydrous zinc chloride was added into the flask as quickly as possible at 323 K. After the added zinc chloride was dissolved completely, the reaction mixture was evenly heated to 388 K within 1 h. After holding the reaction for about 8 h at 388 K, the polymeric beads HJ-Y10 were separated from the reaction solution and rinsed by 1% of hydrochloric acid (v/v) and ethanol in turn for three times, then they were extracted by ethanol for 8 h and dried at 323 K in vacuum.

2.3. Characterization of HJ-Y10 resin

Specific surface area and pore diameter distribution of the resin was determined via N_2 adsorption–desorption curves at 77 K using a Micromeritics Tristar 3000 surface area and porosity analyzer. FT-IR spectrum of the resin was collected by KBr disks on a Nicolet 510P Fourier-transformed infrared instrument.

2.4. Adsorption isotherms

About 0.100 g of the resin was weighed accurately and added into a 100 mL of conical flask with a stopper, and 50 mL of *p*-aminobenzoic acid aqueous solution with known initial concentration was also added into the flask. The initial concentration of *p*-aminobenzoic acid was 100–500 mg/L with 100 mg/L interval. Hydrochloric acid and sodium hydroxide were applied to adjust the solution pH. Then the flask was shaken at a speed of 150 rpm at a desired temperature for about 24 h. After the adsorption system reached equilibrium, concentration of the equilibrium *p*-aminobenzoic acid solution was measured by UV spectrometry at a wavelength of 266.0 nm and the equilibrium adsorption capacity was calculated as [26]:

$$q_e = \frac{(C_0 - C_e)V}{W} \quad (1)$$

where q_e was the equilibrium adsorption capacity (mg/g), C_0 and C_e were the initial and equilibrium concentration of *p*-aminobenzoic acid (mg/L), V was the volume of the solution (L), and W was the mass of the resin (g).

2.5. Adsorption kinetic curves

To take consideration of the effect of the adsorption time on the adsorption capacity of *p*-aminobenzoic acid onto the resin and the adsorption kinetic curves were measured as follows. About 1.000 g of resin and 500 mL of *p*-aminobenzoic acid solution were introduced into a conical flask quickly and shaken at a speed of 150 rpm at 299, 309 and 319 K continuously. 0.5 mL of solution was sampled at different time intervals and concentration of the residual *p*-aminobenzoic acid was determined until adsorption equilibrium was reached, the adsorption capacity at contact time t was calculated as [26]:

$$q_t = \frac{(C_0 - C_t)V}{W} \quad (2)$$

here q_t and C_t was the adsorption capacity and concentration of *p*-aminobenzoic acid at contact time (min) in the unit of (mg/g) and (mg/L), respectively.

3. Results and discussion

3.1. Characterization of HJ-Y10 resin

Specific surface area and pore volume of HJ-Y10 resin was measured to be 440.2 m^2/g and 0.206 cm^3/g, respectively. Fig. s1(a) describes the N_2 adsorption–desorption isotherms of HJ-Y10 resin. The adsorption isotherm seems close to type-II isotherm [30]. At the initial part of the isotherm at a relative pressure below 0.10, the adsorption capacity increases rapidly with increment of relative pressure, proving that micropores are existent (t-plot micropore area: 221.8 m^2/g, t-plot micropore volume: 0.121 cm^3/g). The visible hysteresis loop of the desorption isotherm indicates that mesopores are also present. These analyses agree with the pore diameter distribution in Fig. s1(b). Friedel-Crafts reaction leads many changes for pore diameter distribution, mesopores and macropores dominate pore structure for chloromethylated PS and the average pore diameter is 25.2 nm, while mesopores in the range of 2–5 nm play a predominant role for HJ-Y10 resin and the average pore diameter is 2.81 nm.

As displayed in Fig. 1, after Friedel-Crafts reaction, two strong representative peaks related to CH_2Cl groups at 1265.1 and 669.2 cm^{-1} are greatly weakened, and Friedel-Crafts reaction results in a few new changes for the IR spectrum of HJ-Y10 resin. Firstly, a moderate C=O stretching band involved in formaldehyde carbonyl groups comes forth at 1699.2 cm^{-1}, and appearance of this band may be from oxidation of benzyl chloride of chloromethylated PS [31]. The second change can be seen that a moderate vibration presents at 1654.8 cm^{-1}, and which can be assigned to C=O stretching concerned with quinone carbonyl groups [32]. This implies the uploaded hydroquinone on the resin is partly oxidized. Finally, a weak absorption band appears at 3530.5 cm^{-1}, and this band is related to O–H stretching of hydroquinone.

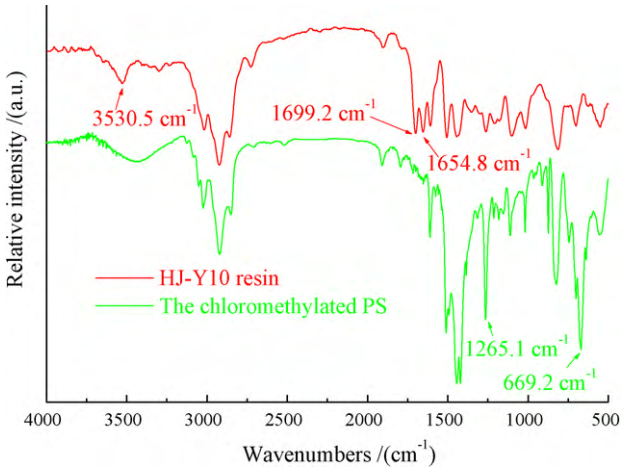

Fig. 1. FT-IR spectra of the chloromethylated PS and HJ-Y10 resin.

3.2. Comparison of adsorption capacity of p-aminobenzoic acid

The adsorption capacities of *p*-aminobenzoic acid adsorbed onto HJ-Y02, HJ-Y06, HJ-Y10 and HJ-Y15 (the added mass percentage of hydroquinone in the Friedel-Crafts reaction was set to 2%, 6%, 10% and 15% in relation to the chloromethylated PS, w/w) are compared in Fig. s2. It is seen that the adsorption capacity of *p*-aminobenzoic acid firstly increases and then decreases with increment of the added mass percentage of hydroquinone. The specific surface areas (395.6, 379.1, 404.2 and 446.3 m^2/g) and the average pore diameter (2.90, 2.92, 2.81 and 2.78 nm) of these four resins are close, and the different adsorption capacity shows their different polarity matching between the adsorbent and the adsorbate [17,27]. HJ-Y10 resin holds the largest adsorption capacity for *p*-aminobenzoic acid among the four resins and it is applied to investigate the adsorption behaviors for *p*-aminobenzoic acid in the subsequent sections.

3.3. Effect of the solution pH on the adsorption

Fig. 2 displays effect of the solution pH on adsorption of *p*-aminobenzoic acid onto HJ-Y10 resin. It is seen that the adsorption is very sensitive to the solution pH and the optimum solution pH is observed at 3.79. In this study, the pH of *p*-aminobenzoic acid solution is measured to be 3.79 (the pK_a of *p*-aminobenzoic acid was 4.92). That is, *p*-aminobenzoic acid is a weak acid and has its own ionization equilibrium (Scheme s2), it will be ionized to be a negative ion as the solution pH is higher than 3.79, whereas the amino group will accept a proton and it will be presented as a positive ion as the solution pH is lower than 3.79. The fact that the maximum adsorption capacity of *p*-aminobenzoic acid presents at solution pH of 3.79 indicates that molecular form of *p*-amniobenzoic acid is suitable for the adsorption [33]. In addition, it is observed that the adsorption is greatly reduced as the pH is higher or lower than 3.79, and the basic solution (pH > 6.0) is especially unfavorable for the adsorption, which reveals that the carboxyl group of *p*-amniobenzoic acid is important for the adsorption, and this in turn implies that the formaldehyde carbonyl and quinone carbonyl groups on HJ-Y10 resin are helpful for the adsorption.

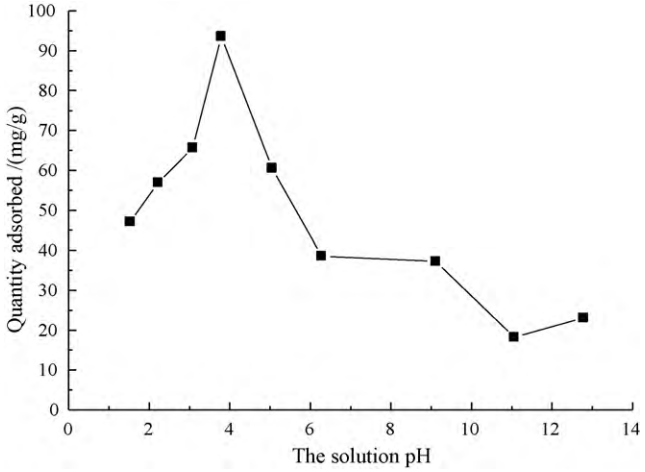

Fig. 2. Effect of the pH on the adsorption of *p*-aminobenzoic acid onto HJ-Y10 resin from aqueous solution (the adsorption time was 24 h, the volume was 50 mL, the concentration of *p*-aminobenzoic acid was 499.8 mg/L, the shaking speed was 150 rpm and the temperature was 299 K, 0.1 mol/L of hydrochloric acid and 0.1 mol/L of sodium hydroxide were applied to adjust the pH).

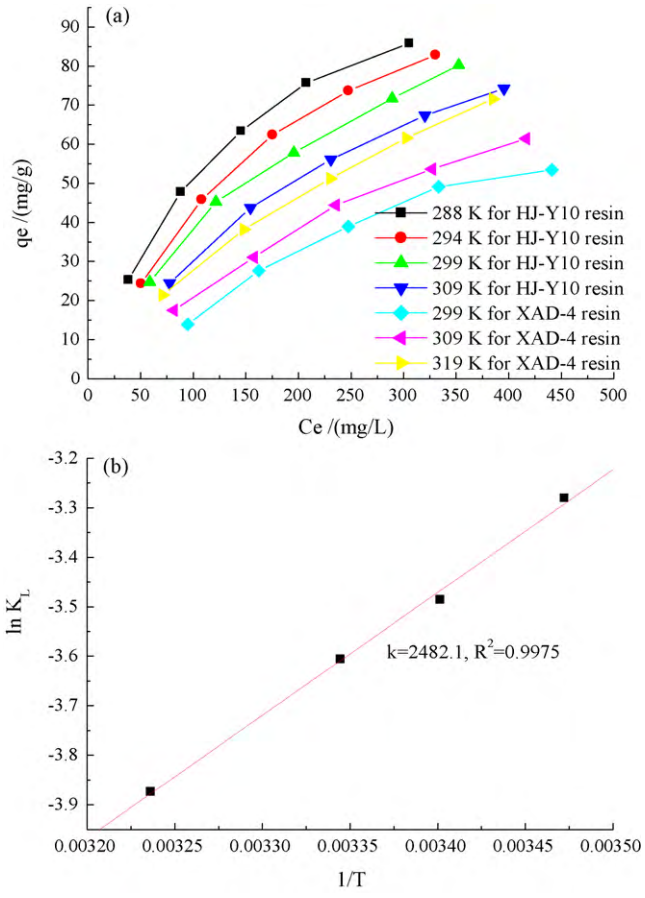

Fig. 3. (a) Adsorption isotherms of *p*-aminobenzoic acid onto HJ-Y10 resin from aqueous solution with the temperature at 288, 294, 299 and 309 K and that of *p*-aminobenzoic acid onto XAD-4 resin at 299, 309 and 319 K (the initial concentration of was *p*-aminobenzoic acid set to be about 100, 200, 300, 400 and 500 mg/L, the pH was not adjusted); (b) correlation of ln K_L with 1/T for the adsorption of *p*-aminobenzoic acid onto HJ-Y10 resin from aqueous solution.

3.4. Adsorption isotherms and adsorption thermodynamics

Fig. 3(a) shows the adsorption isotherms of *p*-aminobenzoic acid onto HJ-Y10 resin together with that onto the popular commercial XAD-4 resin. The adsorption capacity of *p*-aminobenzoic acid onto HJ-Y10 decreases with increasing of the temperature and higher temperature is less favorable for the adsorption, suggesting that the adsorption is an exothermic process for HJ-Y10 resin [34]. While the adsorption onto XAD-4 resin is more favored at a higher temperature, enunciating an endothermic process [34]. Additionally, it is observed that the adsorption capacity of *p*-aminobenzoic acid onto

HJ-Y10 resin is a bit larger than that onto XAD-4 resin at the same temperature and equilibrium concentration.

Langmuir and Freundlich isotherm models are frequently adopted to describe the adsorption process. Langmuir isotherm model:

$$\frac{C_e}{q_e} = \frac{C_e}{q_m} + \frac{1}{q_m \times K_L} \tag{3}$$

Freundlich isotherm model:

$$\log\ q_e = \log K_F + \frac{1}{n} \log C_e \tag{4}$$

where q_m is the maximum adsorption capacity (mg/g), and K_L (L/mg), K_F, and n is the corresponding characteristic constants. In the present study, Langmuir and Freundlich isotherm models are employed to describe the adsorption equilibrium data, the fitted plots are shown in Fig. s3 and the corresponding parameters K_L, K_F and n, correlation coefficients R^2 are summarized in Table s1. All of the isotherms coincide with the fitted results based on Langmuir model since $R^2 > 0.99$. With increasing of the temperature, K_L and q_m decrease, implying weaker adsorption driving force and the smaller adsorption capacity at a higher temperature.

The thermodynamic parameters such as adsorption enthalpy ΔH (kJ/mo1), adsorption free energy ΔG (kJ/mo1) and adsorption entropy ΔS (J/(mo1 K)) can be calculated as [35]:

$$\ln\ K_L = -\frac{\Delta H}{RT} + \ln K_0 \tag{5}$$

$$\Delta G = -RT\ \ln K_L \tag{6}$$

$$\Delta S = \frac{\Delta H - \Delta G}{T} \tag{7}$$

where R is the universal gas constant, 8.314 J/(mol K), T is the absolute temperature (K) and K_0 is a constant. By plotting $\ln K_L$ versus $1/T$ (Fig. 3(b)), a straight line is gained, and ΔH can be figured out from the slope of the straight line. As listed in Table s2, the negative ΔH and ΔS reveal the adsorption is mainly driven by enthalpy change and the adsorption of *p*-aminobenzoic acid onto HJ-Y10 resin is an exothermic and more ordered process.

3.5. Adsorption kinetics

Fig. 4(a) shows the adsorption kinetic curves for *p*-aminobenzoic acid adsorbing on HJ-Y10 and XAD-4 resin. All of the adsorption process can approach equilibrium within 400 min, and the adsorption at a lower initial concentration or higher temperature needs shorter time to reach at equilibrium but achieves smaller adsorption capacity. As for the comparison of HJ-Y10 with XAD-4 resin, it is clear that the adsorption capacity of *p*-aminobenzoic acid on HJ-Y10 resin is a little larger than XAD-4 resin at the same temperature and initial concentration while the required time is a little longer than XAD-4 resin.

Lagergren equation is frequently applicable for depicting the adsorption in the beginning process and not the whole one [36], while pseudo-second-order rate equation by Ho is suitable for describing the whole process [37], and its linear form is:

$$\frac{t}{q_t} = \frac{1}{k_2 \times q_e^2} + \frac{t}{q_e} \tag{8}$$

here k_2 is the pseudo-second-order rate constant (g/(mg min)). The fitted results in Table s3 indicate that the pseudo-second-order rate equation can characterize the adsorption well. In particular, the rate constant at a lower initial concentration or higher temperature is a little greater, accordant with the above observation that the adsorption at a lower initial concentration or higher temperature needs shorter time to reach at equilibrium. Additionally, based on the pseudo-second-order rate equation, the initial adsorption rate

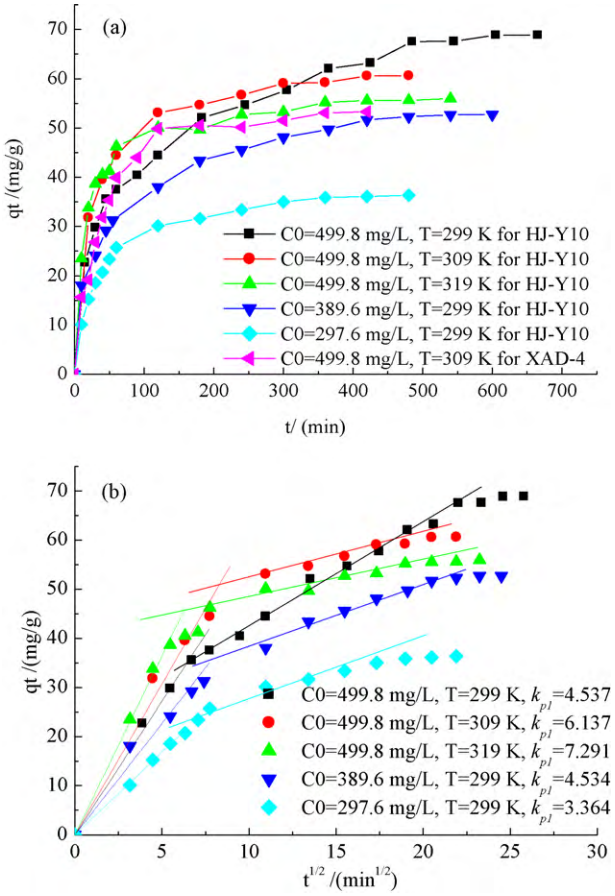

Fig. 4. (a) Adsorption kinetic curves of *p*-aminobenzoic acid adsorbed onto HJ-Y10 and XAD-4 resin (the volume was 500 mL, the pH was not adjusted, 0.5 mL of *p*-aminobenzoic acid solution was sampled at different intervals); (b) intra-particle diffusion plot for the adsorption of *p*-aminobenzoic acid onto HJ-Y10 resin from aqueous solution.

(h) with unit of mg/(g min) and half-adsorption time ($t_{1/2}$) with unit of min can be calculated as:

$$h = k_2 q_e^2 \tag{9}$$

$$t_{1/2} = \frac{1}{k_2 q_e} \tag{10}$$

The data summarized in Table s3 shows that the h is greater while the $t_{1/2}$ is shorter at a higher temperature. For the kinetic curves at different temperatures, the apparent activation energy E_a (kJ/mol) can be calculated based on the Arrhenius equation as:

$$\ln\ k_2 = -\frac{E_a}{RT} + \ln k_0 \tag{11}$$

where k_0 is a constant. Plotting of $\ln k_2$ versus $1/T$, a straight line will be obtained, and E_a can be achieved to be 61.38 kJ/mol.

In general, several steps including external mass transfer from the liquid solution to the solid resin surface, internal mass transfer in the pore of the resin, and adsorption on the active sites of the resin are necessary for the adsorbate transporting from the liquid solution to the active sites of the resin, and the rate of internal mass transfer is commonly the rate controlling step. The intra-particle diffusion model proposed by Weber and Morris is applied to further fit the kinetic results in the present study [38]. The rate of intra-particular diffusion is a function of $t^{1/2}$ and can be defined as:

$$q_t = k_p \times t^{1/2} \tag{12}$$

here k_p is the diffusion rate parameter ([(mg/g)/(min)$^{1/2}$]) and can be figured out by plotting of q_t versus $t^{1/2}$. If intra-particle diffu-

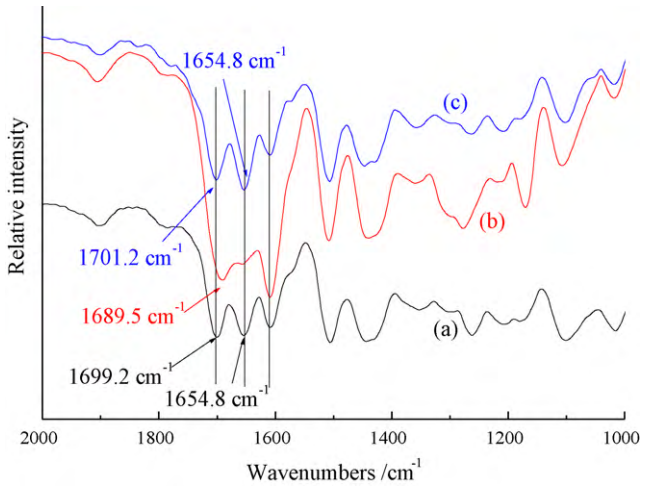

Fig. 5. FT-IR spectrum of HJ-Y10 resin: (a) before adsorption of *p*-aminobenzoic acid (the original HJ-Y10 resin); (b) after adsorption of *p*-aminobenzoic acid; (c) after the adsorbed *p*-aminobenzoic acid on HJ-Y10 resin was desorbed.

sion is involved in the adsorption process, plotting of q_t versus $t^{1/2}$ will give a linear relationship, and if this line passes through the origin, the intra-particle diffusion is the sole rate controlling step.

Fig. 4(b) depicts the intra-particle diffusion plots for the adsorption of *p*-aminobenzoic acid on HJ-Y10 resin. These plots show similar characters having two linear segments followed by a plateau. In the first stage, the linear portion passes through the origin, implying that the intra-particle diffusion is the sole rate controlling step, and the k_p evaluated from the first linear portions are 4.537, 6.137 and 7.291, 4.534 and 3.364, respectively. In the following stage, the regression is approximately linear but does not pass through the origin, suggesting that the intra-particle diffusion is not the sole rate controlling step in this stage. After that, the adsorption reaches equilibrium.

3.6. Interaction mechanism between HJ-Y10 resin and *p*-aminobenzoic acid

The vibrational frequency in FT-IR spectrum is sensitive to the change of chemical bond, a slight interaction change between the adsorbent and the adsorbate will bring on several vibrational shifts [39]. In this study, FT-IR spectrum is utilized to examine the shifts of formaldehyde carbonyl and quinone carbonyl groups on HJ-Y10 resin so that the adsorption mechanism can be clarified. The typical results of HJ-Y10 resin before adsorption, after adsorption and after desorption of *p*-aminobenzoic acid are depicted in Fig. 5. The two main peaks of HJ-Y10 resin before adsorption can be assigned as: 1699.2 cm^{-1} (formaldehyde carbonyl groups) and 1654.8 cm^{-1} (quinone carbonyl groups). After adsorption of *p*-aminobenzoic acid, the formaldehyde carbonyl has its frequency at 1689.5 cm^{-1}, red-shifted by 9.7 cm^{-1}, the vibration of quinone carbonyl is flat. Moreover, after the adsorbed *p*-aminobenzoic acid on HJ-Y10 resin is desorbed, these two peaks come back to 1701.2 and 1654.8 cm^{-1}, respectively. As for some other vibrations like that of C=C bond at 1606.4 and 1506.3 cm^{-1}, not any shifts are observed. Commonly, formation of hydrogen bonding will lead some characteristic bands to be red-shifted [40]. We deduce that hydrogen bonding appears to be one of the primary driving forces for the adsorption of *p*-aminobenzoic acid onto HJ-Y10 resin and hydrogen bonding is one of the primary driving forces for the adsorption.

4. Conclusions

We have synthesized a novel hyper-cross-linked resin HJ-Y10, its surface is chemically modified by formaldehyde carbonyl, quinone carbonyl and phenolic hydroxyl groups. The adsorption of *p*-aminobenzoic acid on HJ-Y10 is favorable at the solution pH of 3.79. Langmuir model depicts the isotherms well, and the adsorption enthalpy and adsorption entropy are both negative. The pseudo-second-order rate equation characterizes the kinetic curves well and the intra-particle diffusion model is the sole rate controlling step at the initial stage. Formaldehyde carbonyl and quinone carbonyl groups of HJ-Y10 resin are helpful for the adsorption and hydrogen bonding appears to be one of the primary driving forces for the adsorption.

Acknowledgments

The research was supported in part by the National Natural Science Foundation of China (No. 20804058), the undergraduate innovative experiment project in Changsha University and the Science Foundation of Changsha University.

Appendix A. Supplementary data

Supplementary data associated with this article can be found, in the online version, at doi:10.1016/j.cej.2010.05.017.

References

[1] R.A. Brain, A.J. Ramirez, B.A. Fulton, C.K. Chambliss, B.W. Brooks, Herbicidal, Environ. Sci. Technol. 42 (2008) 8965.
[2] A.F. Lago, J.Z. Davalos, A.N. de Brito, Chem. Phys. Lett. 443 (2007) 232.
[3] A.K. Hunter, G. Carta, J. Chromatogr. A 971 (2002) 105.
[4] I. Turku, T. Sainio, Sep. Purif. Technol. 69 (2009) 185.
[5] H.L. Wang, Z.H. Fei, J.L. Chen, Q.X. Zhang, Y.H. Xu, J. Environ. Sci. 19 (2007) 1298.
[6] A.K. Hunter, G. Carta, J. Chromatogr. A 897 (2000) 65.
[7] S.H. Lin, R.S. Juang, J. Environ. Manage. 90 (2009) 1336.
[8] E.X. Perez-Almodovar, G. Carta, J. Chromatogr. A 1216 (2009) 8339.
[9] T. Sainio, M. Laatikainen, E. Paatero, Fluid Phase Equilibr. 218 (2004) 269.
[10] V.A. Davankov, M.P. Tsyurupa, React. Polym. 13 (1990) 27.
[11] V.A. Davankov, S.V. Rogozhin, M.P. Tsyurupa, Macrocrosslinked Polystyrenes, US Patent Appl. 3 (1971) 729.
[12] C.F. Chang, C.Y. Chang, K.E. Hsu, S.C. Lee, W. Hoell, J. Hazard. Mater. 155 (2008) 295.
[13] J.Y. Tseng, C.Y. Chang, C.F. Chang, Y.H. Chen, C.C. Chang, D.R. Ji, C.Y. Chiu, P.C. Chiang, J. Hazard. Mater. 171 (2009) 370.
[14] N. Fontanals, J. Cortes, M. Galia, R.M. Marce, P.A.G. Cormack, F. Borrull, D.C. Sherrington, J. Polym. Sci. A 43 (2005) 1718.
[15] N. Fontanals, P.A.G. Cormack, D.C. Sherrington, J. Chromatogr. A 1215 (2008) 21.
[16] N. Fontanals, M. Galia, P.A.G. Cormack, R.M. Marce, D.C. Sherrington, F. Borrull, J. Chromatogr. A 1075 (2005) 51.
[17] A.M. Li, Q.X. Zhang, G.C. Zhang, J.L. Chen, Z.H. Fei, F.Q. Liu, Chemosphere 47 (2002) 981.
[18] D. Bratkowska, R.M. Marce, P.A.G. Cormack, D.C. Sherrington, F. Borrull, N. Fontanals, J. Chromatogr. A 1217 (2010) 1575.
[19] C. Valderrama, J.I. Barios, M. Caetano, A. Farran, J.L. Cortina, React. Funct. Polym. 70 (2010) 142.
[20] Q.W. Wang, Y.C. Yang, H.B. Gao, Problems on Hydrogen Bonding in Organic Chemistry, Tianjin University Press, Tianjin, 1993.
[21] A.J. Glemza, K.L. Mardis, A.A. Chaudhry, M.K. Gilson, G.F. Payne, Ind. Eng. Chem. Res. 39 (2000) 463.
[22] M.C. Xu, C.R. Wang, Z.Q. Shi, M.C. Xu, S. Zhang, H.T. Li, Y.G. Fan, B.L. He, Chin. J. React. Polym. 9 (2000) 17.
[23] N. Maity, G.F. Payne, Langmuir 7 (1991) 1241.
[24] J.H. Huang, Y. Zhou, K.L. Huang, S.Q. Liu, Q. Luo, M.C. Xu, J. Colloid Interface Sci. 316 (2007) 10.
[25] N. Maity, G.F. Payne, J.L. Chipchosky, Ind. Eng. Chem. Res. 30 (1991) 2456.
[26] J.H. Huang, K.L. Huang, C. Yan, J. Hazard. Mater. 167 (2009) 69.
[27] J.H. Huang, K.L. Huang, S.Q. Liu, Q. Luo, S.Y. Shi, J. Colloid Interface Sci. 317 (2008) 434.
[28] B.J. Brune, J.A. Koehler, P.J. Smith, G.F. Payne, Langmuir 15 (1999) 3987.
[29] D.A. Perry, J.S. Cordova, L.G. Smith, H.J. Son, E.M. Schiefer, E. Dervishi, F. Watanabe, A.S. Biris, J. Phys. Chem. C 113 (2009) 18304.
[30] M. El-Merraoui, H. Tamai, H. Yasuda, T. Kanata, J. Mondori, K. Nadai, K. Kaneko, Carbon 36 (1998) 1769.

[31] G.H. Meng, A.M. Li, W.B. Yang, F.Q. Liu, X. Yang, Q.X. Zhang, Eur. Polym. J. 43 (2007) 2732.
[32] J.T. Wang, Q.M. Hu, B.S. Zhang, Y.M. Wang, Organic Chemistry, Nankai University Press, Tianjing, 1998.
[33] J.H. Huang, X.M. Wang, X. Deng, J. Colloid Interface Sci. 337 (2009) 19.
[34] B.L. He, W.Q. Huang, Ion Exchange and Adsorption Resin, Shanghai Science and Technology Education Press, Shanghai, 1995.
[35] B.C. Pan, W.M. Zhang, B.J. Pan, H. Qiu, Q.R. Zhang, Q.X. Zhang, S.R. Zheng, Environ. Sci. Technol. 42 (2008) 7411.
[36] S. Lagergren, Zur, theorie der sogenannten adsorption geloster stoffe, K. Sven. Vetenskapsakad. Handl. 24 (1898) 1.
[37] Y.S. Ho, G. McKay, Sorption of dye from aqueous solution by peat, Chem. Eng. J. 70 (1998) 115.
[38] W.J. Weber, J.C. Morris, J. Sanit. Eng. Div. Am. Soc. Civ. Eng. 89 (1963) 31.
[39] J.A. Koehler, K.K. Wallace, P.J. Smith, G.F. Payne, Ind. Eng. Chem. Res. 38 (1999) 3076.
[40] M.C. Xu, Z.Q. Shi, M.C. Xu, J.Z. Li, J.X. Sun, B.L. He, Chin. J. React. Polym. 9 (2000) 1.